

Translational Diffusion, Relaxation Times, and Quasi-Elastic Scattering of Flexible Chains with Excluded Volume and Fluctuating Hydrodynamic Interactions. A Brownian Dynamics Study

Antonio Rey and Juan J. Freire*

Departamento de Química Física, Facultad de Ciencias Químicas, Universidad Complutense, 28040 Madrid, Spain

José García de la Torre

Departamento de Química Física, Facultad de Ciencias Químicas y Matemáticas, Universidad de Murcia, 30071 Murcia, Spain

Received October 17, 1990; Revised Manuscript Received March 4, 1991

ABSTRACT: A polymer model with excluded volume interactions represented by a relatively soft potential is employed in Brownian dynamics simulations. The model and method have been shown in previous work to reproduce equilibrium properties and diffusion coefficients calculated with preaveraged hydrodynamic interactions. Trajectories obtained with fluctuating hydrodynamic interactions are now analyzed to obtain the diffusion coefficient, relaxation times of the Rouse coordinates, and the quasi-elastic scattering form factor, together with its first cumulant, of chains with different numbers of units. The main conclusions are as follows: an abnormal increase of the diffusion coefficient with respect to its preaveraged value for the shortest chains, tentatively attributed to effects in the relatively large surface of conformations with overlapping units. These effects seem to be eliminated through extrapolations to the long-chain limit. Thus, the extrapolated ratio of the radius of gyration to the hydrodynamic radius is higher than the estimations for unperturbed Gaussian chains and is in good agreement with upper and lower bounds. The relaxation times are consistently higher than those obtained for Gaussian chains. The results for the cumulants are generally lower than those predicted by Benmouna and Akcasu, the differences being attributed to the lack of consistency between the blob model and the chain models with long-range interactions employed in simulation work. Finally, the Pecora procedure to extract diffusion coefficients and relaxation times from the quasi-elastic form factor is favorably tested for the case of excluded volume chains.

Introduction

The dynamics of a flexible chain in a continuous solvent has been the object of great interest from the theoretical point of view.¹ Perhaps the major difficulty in describing this dynamic is to find an adequate mathematical treatment of the fluctuating hydrodynamic interactions (FHI) between polymer units. Recently, Brownian dynamics (BD) simulations have been performed in order to check the theoretical approximations that try to overcome this problem. For instance, BD has been applied to the correct prediction of diverse properties of linear chains such as fluorescence anisotropy,² polarized^{3,4} and depolarized² quasi-elastic light scattering, and hydrodynamic properties.⁵ An analysis of the Rouse internal motions of the chains, which have a major influence on many properties, have also been performed.³ However, these studies considered chains without long-range intramolecular interactions, which constitutes good representations of real polymers only in the unperturbed or θ conditions, because of the difficulties in introducing such interactions. Thus, BD simulations for chains with excluded volume (EV) have only been attempted to predict equilibrium properties, neglecting hydrodynamic interactions.⁶

The dynamics of chains under the EV or good solvent conditions, for which most universal features of polymers are manifested, have only been described through theories that contain approximate hydrodynamic treatments, such as the popular preaveraged hydrodynamic interactions (PHI) procedure.^{1,7} Also, we should mention some numerical investigations of polymer dynamics based on the Monte Carlo (MC) method,⁸ though this method does not admit an easy introduction of hydrodynamic interactions. Consequently, only in the case of hydrodynamic properties are they able to provide quantitative estimations of the

dynamic properties (MC calculations have been devised to constitute lower or upper bounds of the real values of these properties with FHI⁹).

In a previous paper¹⁰ (paper 1), we proposed a new model of flexible chains represented by Gaussian units with long-range EV interactions. These interactions are treated as relatively soft potentials so that the useful time scales in which they act along the trajectories are not very different from those of the Rouse entropic potential joining neighboring units. We have shown in paper 1 that this model reproduces remarkably well the equilibrium properties of an equivalent, more conventional, model with hard-sphere EV interactions, studied through a MC method. Furthermore, BD results were also reported there for the diffusion coefficient calculated with PHI. In the present work, we describe the results obtained with this model and FHI for the diffusion coefficient, the relaxation times of the Rouse internal motions, and the quasi-elastic light scattering (QELS) function and its first cumulant. All these results are compared with those obtained for simple Gaussian chains without EV. The effect of introducing FHI or employing PHI as an approximation is also discussed. Moreover, we have extracted values of the diffusion coefficient and the relaxation times from the QELS functions through the numerical methods that are commonly used to treat experimental data. These values are then compared with those obtained directly from the trajectories for the same property in order to check the performance of different treatments of experimental data. Some of the results are also compared with available theoretical predictions.

Method

We have computed BD trajectories for linear chains constituted of N statistical units so that, in the absence of long intramolecular interactions, the distance between neighboring units would follow a Gaussian distribution with a root-mean-square value b . Two types of intramolecular forces are then considered: those due to harmonic springs between first neighbors, described by the usual Rouse potential,⁷ and repulsive forces between non-neighboring units that mimic the EV interactions. The latter forces are introduced by means of a potential of the form $Ae^{-\beta R_{ij}}$, with a cutoff distance r_c . Adequate numerical values of the parameters were investigated in paper 1, a relatively wide range of these values giving a good description of the behavior expected for several equilibrium properties of chains in the excluded volume conditions, as different averages of internal distances and the distribution of the end-to-end distance, also calculated with a Monte Carlo procedure for an equivalent hard-spheres model. In this way, we selected the final values $A = 75.0$, $\beta = 4$, and $r_c = 0.512$, which are also used in the present work, in reduced units (see below). As in earlier simulations,^{3,10} hydrodynamic interactions are also introduced through the diffusion tensor proposed by Rotne and Prager¹¹ and Yamakawa.¹² This tensor is configuration-dependent; i.e., it is able to describe FHI in a realistic way. Trajectories are generated with this scheme of forces and hydrodynamic interactions, using the first-order Erman and McCammon algorithm,^{2,3,10} so that the forces and hydrodynamic interactions are kept constant within a given time step.

In order to evaluate the influence of the hydrodynamic interaction description on the dynamic properties of flexible chains, we have also performed BD simulations with PHI, a usual approximation in the standard theories.⁷ For this purpose, we have employed the preaveraged Oseen tensor,⁷ whose components depend on mean reciprocal averages of distances between pairs of units, $\langle R_{ij}^{-1} \rangle$, calculated in the previous MC simulation with the hard-spheres model. This way, we avoid the approximations included in analytical expressions for these averages, such as the ones provided by the blob model¹³ which, as discussed in paper 1, are not in exact agreement with the simulation results.

We generate five different trajectories for each chain. The trajectories are sufficiently long (each one includes 40 000 time steps) so that an adequate signal-to-noise ratio is achieved, as can be verified from the results for different properties, which correspond to means and uncertainties calculated over these five independent samples. Further details on the model and the simulation techniques can be found in ref 3 and paper I, while in subsequent sections we will give the details on the calculation of different properties. The results are always referred to in the following basic units: b for length, the Boltzmann factor $k_B T$ for energy, and the friction coefficient of a unit, ξ , for friction. This coefficient can be expressed as $\xi = 6\pi\eta_0\sigma$, where η_0 is the solvent viscosity and σ is the friction radius of the Gaussian unit, which we set as $\sigma = 0.256b$. Then $\xi b^2/k_B T$ is the basic unit time. All the reduced quantities are denoted by asterisks.

Diffusion Coefficient

The diffusion coefficient, D_t , of chains with different numbers of units, EV and FHI, has been obtained through the quadratic displacement along the trajectories of the center of masses, characterized by its position vector, R_c :

$$\langle [R_c(t) - R_c(t + \tau)]^2 \rangle = 6D_t\tau \quad (1)$$

where the average extends to all the different values of the time t along the trajectory. This method was favorably tested in paper 1 for the same model through trajectories generated with PHI. It was then verified that the BD results for D_t were essentially the same as those obtained from the preaveraged Kirkwood-Riseman formula in terms of the equilibrium averages $\langle R_{ij}^{-1} \rangle$ (eq 3 of paper 1). The BD results obtained with FHI can be found in Table I. We also include in Table I the preaveraged results obtained from the Kirkwood-Riseman formula with distance averages evaluated from the trajectories analyzed in paper

Table I
Translational Diffusion Coefficients (in Reduced Units)
Obtained by Different Methods for an Excluded Volume
Chain of Varying Numbers of Units^a

N	D_0^*	$(D_t^*)_{BD}$	$(D_t^*)_P$	$D_0^* - D_1^*$	$(D_t^*)_Z^b$
6	0.357	0.398 ± 0.004	0.355	0.352	0.340
8	0.302	0.335 ± 0.002	0.300	0.297	0.286
11	0.252	0.262 ± 0.002	0.250	0.247	0.236
15	0.211	0.231 ± 0.002	0.209	0.207	0.196
20	0.180	0.186 ± 0.002	0.178	0.176	0.166
25	0.160	0.166 ± 0.002	0.158	0.155	0.145

^a D_0 , results from the Kirkwood formula, eq 2. BD, results from eq 1 calculated from the trajectories. P, results from the Kirkwood-Riseman (preaveraged) formula. Z, Monte Carlo values from the Zimm (lower bound) method. D_1 is defined in the text. ^b Error <0.001 in all cases.

1. Moreover, we include results obtained with the same averages for D_0 , the diffusion coefficient obtained from the well-known, though also approximate, Kirkwood formula⁷

$$D_0 = (k_B T / N\xi) [1 + (\sigma/N) \sum_i \sum_j \langle R_{ij}^{-1} \rangle] \quad (2)$$

The results in Table I are somehow surprising, since one should expect that $D_t = D_0 - D_1$, where D_1 is positive, with a lower bound constituted by its preaveraged value.^{9,11} However, we observe that $D_t > D_0$. According to Fixman,⁵ D_1 can be independently calculated from the trajectories as

$$D_1 = (1/3N) \int_0^\infty C_A(\tau) d\tau \quad (3)$$

where

$$C_A(\tau) = \langle \mathbf{A}(t) \cdot \mathbf{A}(t + \tau) \rangle \quad (4)$$

and

$$\mathbf{A} = (1/k_B T) \sum_i \sum_j \mathbf{H}_{ij} \mathbf{F}_j \quad (5)$$

where $\mathbf{H} = \mathbf{D}/(k_B T)$, \mathbf{D} being the diffusion tensor and \mathbf{F}_j the intramolecular force on unit j . We have performed the calculation for D_1 from the trajectories with FHI and PHI. The ratio of the values of $C_A(t)$ obtained through these two different hydrodynamic treatments is shown in Figure 1 for different chain lengths. It can be observed that this ratio is always greater than 1, in accordance with the prediction of a preaveraged lower bound for D_1 . Moreover, the ratios closely follow the trends observed by Fixman for Gaussian chains,⁵ with a peak at $t = 0$ and approaching the value 1 relatively rapidly, which constitutes its asymptotic long-time limit. Furthermore, since the decay of these correlation functions is fast, we have been able to estimate the integrated value of D_1 , which in all cases represents only a few percent of D_0 (it is even smaller than the D_1 contribution for Gaussian chains calculated previously by Fixman⁵). The values of $D_0 - D_1$ obtained with PHI are practically identical with the Kirkwood-Riseman results, while the values obtained with FHI are included in Table I for comparison with the other estimation for D_t . According to the preceding paragraphs, they are always slightly smaller than D_0 and the preaveraged results, and therefore, they are in contradiction with the numerical values of D_t obtained from eq 1.

Therefore, we have found a disagreement between the results for D_t obtained from eq 1 and those calculated as $D_0 - D_1$. Since the values of D_0 and D_1 seem to be

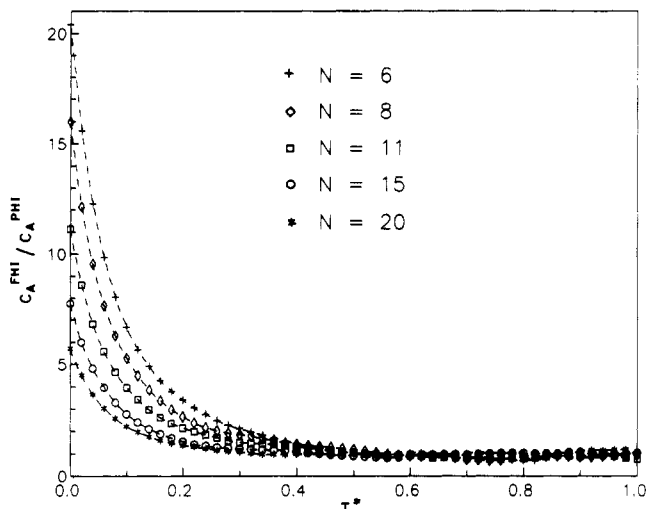


Figure 1. Ratio of the time-correlation function $C_A(\tau)$ defined in eq 4 calculated with FHI to that obtained with PHI for chains of different numbers of units.

reasonable and follow essentially the trend that one should expect from the results for Gaussian chains, we have concentrated our tests on the displacement of the center of masses procedure. The only apparent source of serious bias in the numerical calculations could be the choice of an overly large time step. In paper 1, we showed that given the relatively soft EV potential in our model, we could maintain a value for this interval similar to that employed for Gaussian chains, $\Delta t^* = 0.01$ (in reduced units), without affecting the equilibrium properties or the values of D_t obtained from eq 1 with PHI. The only remaining doubt is whether the presence of important FHI for conformations with overlapping units that cannot be avoided with this time step can somehow distort the dynamics. However, we have reduced the time interval to $\Delta t^* = 10^{-4}$ (increasing the number of steps by the same factor so that the trajectory length remained unchanged) for the chain of 6 units, where the differences are higher, without finding any significant change in the results for D_t with FHI.

Finally, we have reached a possible explanation for these disagreements. Following Fixman,⁹ the average velocity of the center of masses in the presence of an external field \mathbf{E} is obtained from equilibrium averages as

$$\langle \mathbf{v}_c \rangle_E = \langle \mathbf{H} \rangle \mathbf{E} - k_B T \langle \mathbf{H} \Phi \nabla \ln \Phi \rangle \quad (6)$$

where $\Phi = \Psi_E / \Psi$ is the ratio of the perturbed to the equilibrium distribution function. After an integration by parts of the second term on the right-hand side of eq 6, one obtains

$$\langle \mathbf{v}_c \rangle_E = \langle \mathbf{H} \rangle \mathbf{E} + k_B T \langle \Psi^{-1} \Phi \nabla (\mathbf{H} \Psi) \rangle \quad (7)$$

This equation (eq 2.18 in ref 9) leads directly to $D_t = D_0 - D_1$. However, eq 7 implies neglect of surface contributions depending on Ψ_E and the elements H_{ij} . Then, eq 7 is valid if Φ is close to 1 on the configurational surface so that Ψ_E is very small. However, in the case of relatively short chains with EV, Ψ is depressed in the vicinity of overlapping due to a correlation hole effect,¹⁴ while Ψ_E can have a finite value and a contribution may arise for relatively short chains, where the overlapping region is not very small in comparison with the chain volume and the surface of conformations with overlapping units cannot be ignored. Then Φ may be very different from 1 and give a noticeable contribution to the lower boundary of integration of the internal coordinates, corresponding to

Table II
Values of ρ Obtained from the Results for D_t Calculated with the Different Methods Included in Table I^a

N	ρ				
	D_0	BD	P	$D_0 - D_1$	Z^b
6	1.45	1.63 ± 0.03	1.45	1.44	1.41
8	1.48	1.65 ± 0.02	1.47	1.45	1.42
11	1.53	1.59 ± 0.02	1.52	1.48	1.41
15	1.51	1.65 ± 0.02	1.50	1.50	1.41
20	1.53	1.58 ± 0.02	1.51	1.48	1.41
25	1.51	1.59 ± 0.02	1.49	1.48	1.42
∞^c	1.59 ± 0.03	1.54 ± 0.04	1.56 ± 0.03	1.54 ± 0.02	1.41

^a The values of $\langle S^2 \rangle$ are those obtained from the trajectories, except for the Zimm (Z) method, where the Monte Carlo sampling estimates are considered. ^b Error < 0.001 in all cases. ^c Extrapolation from ρ vs $N^{-1/2}$ analysis (poor correlation).

the smallest possible distances between nonneighboring units. This contribution is not significant for PHI, since the preaveraged H_{ij} terms are small for nonneighboring units,⁷ but it can become higher for the FHI which are important for overlapping situations. Then a certain increase of mobility may arise as an effect that should decrease for increasingly longer chains, in qualitative agreement with our simulation results. (A similar conclusion could be reached following the direct derivation of an upper bound for D_t elaborated by Rotne and Prager,¹¹ where the same integration by parts is included.)

Consequently, we conclude that surface effects^{1,11} may be responsible for an abnormal increase of mobility in relatively short chains with excluded volume so that the decrease of D_t due to chain expansion is in part compensated. As the effect decreases for longer chains, we can expect an agreement with the values obtained for $D_0 - D_1$ in the high molecular weight limit. Then, according to our results for D_1 , the results for D_t should be close and slightly smaller than the preaveraged ones, with differences with respect to them smaller than those previously found for Gaussian chains.⁵ These smaller differences can be also shown by comparing the upper bounds for D_t (represented by the preaveraged values) with the lower bounds also included in Table I. The lower bounds have been obtained as means over a Monte Carlo sampling of conformations corresponding to the equivalent hard-spheres model. D_t has been obtained for each conformation by means of a rigorous treatment for rigid bodies. This numerical procedure was first proposed by Zimm¹⁶ and was shown to yield lower bounds for D_t .⁹ Differences between the preaveraged and Zimm values in Table I are not high ($\sim 10\%$, while they are $\sim 15\%$ for Gaussian chains¹⁵). The actual values of D_t should be bracketed by these bounds (once the surface effects are eliminated).

In Table II we show results for ρ , the ratio of the radius of gyration to the hydrodynamic radius, calculated as

$$\rho = \langle S^2 \rangle^{1/2} / (\sigma / D_t^*) \quad (8)$$

It can be observed that this parameter varies slowly with molecular weight, and therefore, it can be tentatively extrapolated to the long-chain limit in a linear regression analysis ρ vs $N^{-1/2}$ for the different hydrodynamic treatments. The extrapolated results are contained in Table II. First, we can notice that ρ is bracketed between the values 1.56 and 1.41 from the lower and upper bounds. The latter value is consistent with the our recent report of calculations with the Zimm method for longer EV chains.¹⁶ The value calculated from eq 1 is now between these limits, though it presents a higher uncertainty range due to a lower correlation caused by finite size effects.

Table III
First and Second Relaxation Times (in Reduced Units) of the Rouse Coordinates or Chains of Different Lengths (with FHI and PHI)

N	FHI		PHI	
	τ_1^*	τ_2^*	τ_1^*	τ_2^*
6	1.41 ± 0.01	0.428 ± 0.009	1.56 ± 0.03	0.434 ± 0.009
8	2.35 ± 0.06	0.691 ± 0.008	2.72 ± 0.07	0.732 ± 0.007
11	4.7 ± 0.1	1.13 ± 0.02	4.8 ± 0.3	1.20 ± 0.02
15	7 ± 0.2	1.79 ± 0.04	7.7 ± 0.2	1.96 ± 0.04
20	11.2 ± 0.2	3.22 ± 0.04	11.9 ± 0.3	3.3 ± 0.2
25	15.0 ± 0.4	4.6 ± 0.1	16.1 ± 0.2	4.7 ± 0.2
β	1.72 ± 0.01	1.67 ± 0.01	1.62 ± 0.01	1.63 ± 0.02

However, it seems to indicate that the surface effects can be eliminated through extrapolation. In fact, the results obtained from $D_0 - D_1$ lead to the same extrapolated value $\rho = 1.54$. This result is between the bounds and is considerably higher than the upper limit value for Gaussian chains calculated by Fixman¹⁷ through an improved lower bound method for D_1 , $\rho = 1.37$. (The preaveraged result for Gaussian chains is⁷ $\rho = 1.48$, which is a poor estimation, though again smaller than the EV result.) These differences between the values of D_i for Gaussian and EV chains are consistent with experimental data (a review of experimental results is provided in ref 16). Moreover, a smaller value of ρ for expanded chains is also predicted by renormalization group theory¹⁸ and attributed to the increase of permeability in expanded coils.

Internal Modes

We have computed the first and second relaxation times, τ_1 and τ_2 , of our chains with long-range intramolecular interactions calculated from the exponential decays of the time correlation functions for the corresponding Rouse coordinates

$$\rho_k(\tau) = \langle \mathbf{u}_k(t) \cdot \mathbf{u}_k(t + \tau) \rangle \quad (9)$$

with

$$\mathbf{u}_k(t) = \sum_j^N (2/N)^{1/2} \cos[(j + 1/2)\pi k/N] \mathbf{R}_j(t) \quad (10)$$

$\mathbf{R}_j(t)$ is the position vector of unit j with respect to an internal frame centered in the center of masses of the chain. The Rouse coordinates represent normal modes of the chains only when hydrodynamic and long-range interactions are absent. FHI and EV make it impossible to work with exact normal motions. However, the standard theory with PHI⁷ and previous simulations with FHI³ have shown that the Rouse coordinates are generally good, though approximate, representations of normal modes.

An exponential behavior of the functions $\rho_k(\tau)$ is theoretically predicted for long times.⁷ Consequently, we have extracted the relaxation times τ_k from least-squares linear fittings of $\ln[\rho_k(\tau)/\rho_k(0)]$ vs τ , in a time range where the numerical errors are kept small. These intervals were selected according to previously described numerical procedures.³ The fitted slopes provide estimations for $(-1/\tau_k)$.

The results for relaxation times (in reduced units) calculated from our BD trajectories with PHI and FHI are contained in Table III. It can be observed that the values obtained with FHI are always slightly smaller than those obtained with PHI. However, differences become smaller for longer chains and is not clear from the present data whether a closer agreement between both sets of results will be reached for the long-chain limit, or the

Table IV
Ratios of Relaxation Times of Excluded Volume (EV) Chains to Those of Gaussian (θ) Chains

N	FHI		PHI ^a	
	$\tau_1^{\text{EV}}/\tau_1^{\theta}$	$\tau_2^{\text{EV}}/\tau_2^{\theta}$	$\tau_1^{\text{EV}}/\tau_1^{\theta}$	$\tau_2^{\text{EV}}/\tau_2^{\theta}$
6	1.15 ± 0.05	1.01 ± 0.04	1.02 ± 0.02	1.05 ± 0.02
8	1.24 ± 0.09	1.03 ± 0.03	1.41 ± 0.04	1.16 ± 0.01
11	1.54 ± 0.06	1.06 ± 0.03	1.54 ± 0.09	1.19 ± 0.02
15	1.43 ± 0.06	1.07 ± 0.03	1.54 ± 0.04	1.23 ± 0.03
20	1.38 ± 0.04	1.21 ± 0.05	1.55 ± 0.04	1.34 ± 0.08

^a The θ values are obtained according to the preaveraged Rouse-Zimm theory.⁷

observed tendencies will be even inverted, as it happens for long Gaussian chains, which show smaller relaxation times when PHI are introduced.³

In Table IV we show a comparison between relaxation times obtained with and without EV interactions. The former times are always greater than the latter, since they exhibit different scaling laws with the number of units. The exponents for $\tau \sim N^{\beta}$ are also included in Table III. In the absence of EV, these exponents were approximately equal to $3/2$, which is the theoretical prediction in θ conditions.⁷ On the other hand, free-draining chains with EV, for which hydrodynamic interactions are neglected, yield⁸ $\beta = 2$. However, it is well-known that the free-draining approximation is too crude and does not provide an adequate description of the dynamic properties even from a qualitative point of view. Our values of β with EV are slightly smaller than the result $\beta = 3\nu$, where ν is the long-chain critical exponent, $\nu = 0.588$.¹⁴

QELS First Cumulant

We have also obtained the first cumulant, $\Omega(q)$, of the quasi-elastic scattering form factor $S(q, \tau)$, defined as

$$\Omega(q) = -[d \ln S(q, \tau)/d\tau]_{\tau=0} \quad (11)$$

In next section we will describe our calculations for $S(q, \tau)$. Nevertheless, due to the possible lack of accuracy related to the numerical evaluation of the derivative in eq 11, we have performed independent calculations for $\Omega(q)$ directly from the trajectories employing a different method, which is now described. This method follows previous theoretical evaluations of the first cumulant based on the formula¹⁹

$$\Omega(q) = \frac{\sum_j^N \sum_k^N \langle (\mathbf{q} \cdot \mathbf{D}_{jk} \cdot \mathbf{q}) \exp(i\mathbf{q} \cdot \mathbf{R}_{jk}) \rangle}{\sum_j^N \sum_k^N \langle \exp(i\mathbf{q} \cdot \mathbf{R}_{jk}) \rangle} \quad (12)$$

To avoid a lengthy calculation employing different orientations with respect to q , an orientational averaging of eq 12 is easily accomplished, yielding the result²⁰

$$\langle \exp(i\mathbf{q} \cdot \mathbf{R}_{jk}) \rangle_{\text{orien}} = \sin(z)/z \quad (13)$$

$$\langle (\mathbf{q} \cdot \mathbf{D}_{jk} \cdot \mathbf{q}) \rangle_{\text{orien}} = q^3 (k_B T / \xi) \{ (\delta_{jk} / q) + (1 - \delta_{jk}) (\xi / 4\pi\eta_0) \times [z^{-2} \sin(z) + z^{-3} \cos(z) - z^{-4} \sin(z)] \} \quad (14)$$

where $z = \mathbf{q} \cdot \mathbf{R}_{jk}$. In the derivation of eqs 13 and 14 no approximations need to be made (the only assumption involves the form of the diffusion tensor); these results correspond to the Oseen tensor with FHI, slightly different from the Rotne-Prager-Yamakawa tensor. However, we believe that this difference should not introduce important inconsistencies in our calculations. The right-hand term of eq 12 is, therefore, directly computed from the trajectories. This way, we avoid any approximation in the

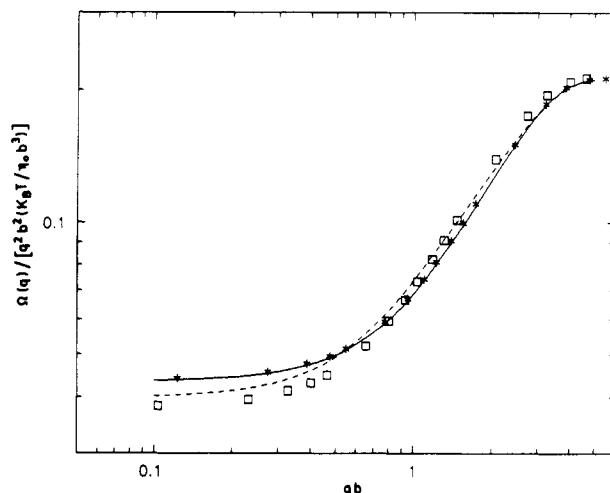


Figure 2. $\Omega(q)/q^2$ vs q (both in reduced units) obtained from our trajectories (points) and from theoretical formulas²¹ (curves) for Gaussian (*, solid) and EV (\square , broken) chains of 20 units, with FHI.

hydrodynamic treatment or in the computation of averaged distances. Consequently, the comparison of our numerical results with those provided by analytical expressions allows us to discern the importance of the different approximations included in the theoretical derivations. We have computed $\Omega(q)$ from BD trajectories with FHI both with and without EV interactions (BD trajectories for Gaussian chains were obtained in previous work, but their cumulant analysis was not then accomplished).

The results obtained for a chain of 20 units for the reduced form of $\Omega(q)/q^2$ vs qb are shown in Figure 2. We have also included the results from an analytical expression derived by Benmouna and Akcasu with FHI,²¹ based in the blob model¹³

$$(\xi b^2/k_B T)\Omega(q) = b^2 q^2 [1 + (3/2)(6/\pi\alpha)^{1/2} J_N(q)] [1 + (2/\alpha) H_N(q)]^{-1} \quad (15)$$

where

$$\alpha = q^2 b^2 / 6$$

and

$$J_N(q) = \alpha \sum_{n=1}^{N-1} (1 - n/N) (1/\alpha n^{2\nu}) [-(\alpha n^{2\nu})^{-1/2} + (2 + 1/\alpha n^{2\nu}) e^{-\alpha n^{2\nu}} \int_0^{(\alpha n^{2\nu})^{1/2}} e^{-t^2} dt] \quad (16)$$

$$H_N(q) = \alpha \sum_{n=1}^{N-1} (1 - n/N) e^{-\alpha n^{2\nu}} \quad (17)$$

(The exponent ν takes the value $\nu = 1/2$ for Gaussian chains and $\nu = 0.588$ when EV conditions are considered. As it is implicit in eqs 15–17, we have identified the blobs with the statistical units in our model.)

We observe in Figure 2 a perfect agreement between the theoretical and simulation results for Gaussian chains. On the other hand, the theoretical results corresponding to EV chains are not coincident with the simulation values. Since the only difference between the analytical derivations for unperturbed and EV chains consists in introducing blob model statistics for the average distances in the latter conditions, the discrepancies indicate a lack of consistency between the blob model and typical EV chain models. As we could see in paper 1, the internal averages of distances between pairs of units in finite size chain models with long-range interactions depend both on the position of

Table V
Results for D_0 Obtained as $\lim_{q \rightarrow 0} \Omega(q)/q^2$ (in Reduced Units)^a

N	D_0 (simulation)		D_0 (theory)	
	θ	EV	θ^b	EV ^c
6	0.387 \pm 0.003	0.366 \pm 0.001	0.385	0.375
8	0.333 \pm 0.003	0.309 \pm 0.001	0.334	0.321
11	0.282 \pm 0.002	0.257 \pm 0.001	0.284	0.270
15	0.244 \pm 0.002	0.2156 \pm 0.0008	0.244	0.227
20	0.211 \pm 0.002	0.1833 \pm 0.0006	0.211	0.194
25		0.162 \pm 0.001	0.189	0.171

^a Calculated from our trajectories and from the Benmouna and Akcasu theory for EV and Gaussian chains (θ) of different number of units. ^b $\nu = 1/2$. ^c $\nu = 0.588$.

the units in the chain backbone and on the chain length, and moreover, they cannot be described by an uniform chain expansion in the EV regime, in contradiction with the blob model assumption. Further discussion on this point will be carried out below.

Three different regions can be considered in the behavior of $\Omega(q)$ vs q shown in Figure 2:

(a) **Small q Region.** At sufficiently small wave vector, characterized by variable x , $x = \langle S^2 \rangle q^2 \ll 1$, both $\Omega(q)$ and $S(q, \tau)$ would reflect exclusively the translational motion contribution to the chain dynamics. In fact, an estimation for the translational diffusion coefficient can be obtained from the first cumulant as

$$D_0 = \lim_{q \rightarrow 0} \Omega(q)/q^2 \quad (18)$$

where D_0 represents again the result obtained from the Kirkwood formula. Consequently, the consideration of FHI or PHI has not effect on the values of D_0 . We have obtained D_0 through eq 18 from the intercept of a least-squares fitting of $\Omega(q)/q^2$ vs q . These values are shown in Table V for the trajectories generated with and without EV interactions. The results for the EV chains are very similar (higher in $\sim 2\%$) to those obtained directly from internal averages through the Kirkwood formula shown in Table I. This constitutes a further verification of the consistency of our numerical methods.

In Table V we have also included the theoretical estimation of D_0 derived from the analytical formulas derived by Benmouna and Akcasu.²² A very good agreement can be observed with our BD results for the Gaussian chains. However, the agreement is poorer for EV chains. The existing discrepancies may be attributed again to the introduction of the blob model in the theoretical derivations. (These differences cannot be attributed to the finite size of our chains since we have also employed the N -dependent theoretical expressions, eqs 28 and 31, of ref 22.) On the other hand, a better agreement can be observed between theoretical and simulation results for the EV chains if the value $\nu = 0.65$ is introduced in the analytical expressions as a substitution for $\nu = 0.588$. However, this unjustified change does not seem to be an adequate way to reconcile theory with simulation.

(b) **Intermediate q Region.** This range of values of q has little utility from the polymer characterization point of view, since it does not provide structural information. However, it has received considerable theoretical attention because a universal dependence of the type $\Omega(q)/q^2 \sim k_B T q / \eta_0$ can be expected. The proportionality constant depends both on the hydrodynamic interactions and on the long-range interactions (or solving conditions). The theoretical values for these constants in the case of long linear chains with FHI are given as²¹ 0.0625 for Gaussian chains (θ conditions) and 0.0789 for EV chains (good

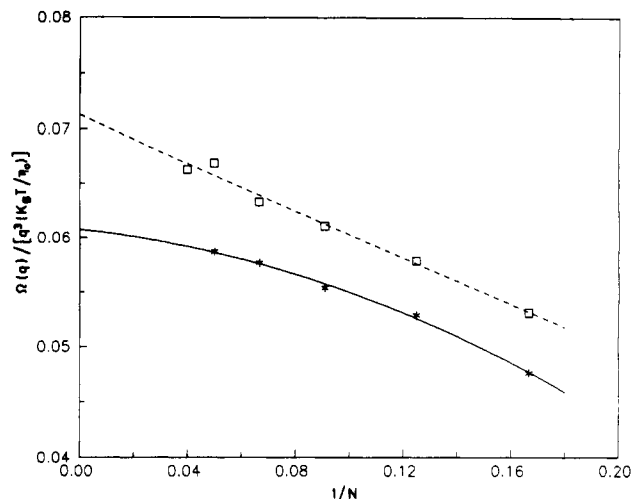


Figure 3. Slope of $\Omega(q)/q^2$ vs q (in reduced units) in the linear region vs $1/N$ for Gaussian (*) and EV (□) chains of different lengths, with FHI. Fitted curves that are employed in the extrapolations to the long-chain limit are also included.

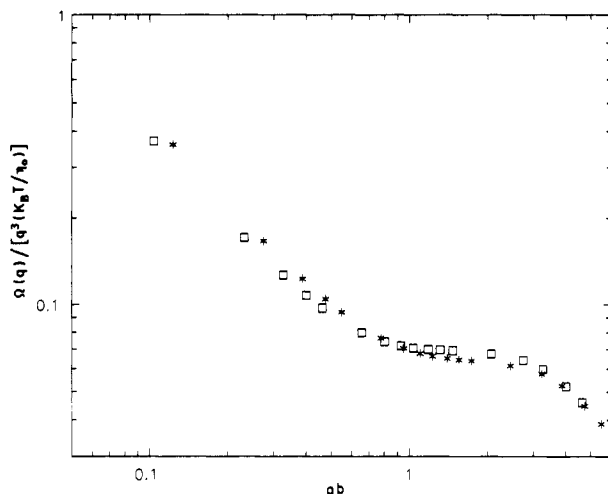


Figure 4. $\Omega(q)/q^3$ vs q (in reduced units) for Gaussian (*) and EV (□) chains of 20 units with FHI.

solvent), values that are considerably higher than the respective results 0.0530 and 0.071 calculated with PHI.

In Figure 3, we show the dependence with chain length of the slopes obtained from a fitting of $\Omega(q)/q^2$ (in reduced units) vs qb in the range of values of q where a linear dependence is observed, i.e., where a plateau is found in a plot of $\Omega(q)/q^3$ vs q (see Figure 4 for the illustration with a chain of 20 units). An extrapolation to $1/N \rightarrow 0$ (by means of an empirically assumed quadratic-type dependence) in Figure 3 allows us to obtain a rough estimation of the slopes in the long-chain limits for both the Gaussian and the EV model from our BD results with FHI. Our results for Gaussian chains lead to a extrapolated value of 0.061, very close to the theoretical result, which is exact for Gaussian chains. This coincidence reinforces the validity of our tentative extrapolations. Then our results for EV chains, 0.071, indicate that the theoretical limit based on the blob model with FHI is too high ($\sim 10\%$ according to the EV chain model employed in this work) so that a fortuitous compensation seems to favor the theoretical treatment based on both the blob model and PHI approximations.

(c) Large q Region. This region is not of great interest from the theoretical point of view, since the expected behavior of the first cumulant is $\Omega(q) = k_B T q^2 / \xi$, corresponding to the diffusion of a single unit of the chain. We have only obtained a few points in this range of values of

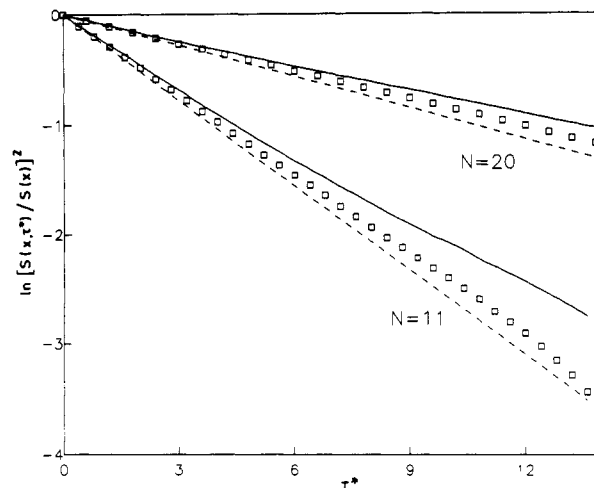


Figure 5. Squared normalized quasi-elastic form factor function vs time (in reduced units) obtained from the trajectories with $x = 1$ for two chains of different lengths with EV. (—) PHI; (□) FHI; (---) initial slopes from the first cumulant analysis.

q , with which we have verified that the single-unit limit has been reached. (Of course, the experimental determination of $\Omega(q)/q^2$ in this plateau region is of great interest for characterizing the chain statistical units.)

Quasi-Elastic Scattering Function

Another dynamic property calculated in this work is the quasi-elastic scattering function or dynamic scattering form factor, defined as²³

$$S(q, \tau) = (1/N^2) \left\langle \sum_j^N \sum_k^N e^{-i\mathbf{q} \cdot [\mathbf{r}_j(t) - \mathbf{r}_k(t + \tau)]} \right\rangle \quad (19)$$

where $\mathbf{r}_l(t)$ represents the position vector of unit l with respect to a external frame, in the t time step of the trajectory. $S(q, \tau)$ should be a real function, and consequently, the evaluation of the imaginary term in eq 19 serves only as an indicator of the statistical noise (or uncertainties) involved in our calculations. For a chain with EV, the formula proposed by Pecora²⁴ for the direct calculation of $S(q, \tau)$ with PHI is not directly applicable since it is based on the Rouse-Zimm distribution function, only valid for Gaussian equilibrium statistics.^{7,23} Consequently, we have evaluated the influence of the preaveraging approximation in $S(q, \tau)$ for EV chains by direct comparison of BD results calculated with FHI and PHI. This comparison is shown in Figure 5 for two different linear chains, with values of q that corresponds to $x = 1$. Systematic differences between the PHI and FHI results are observed. These differences are higher than for Gaussian chains, especially for the shorter chains, and, moreover, exhibit an opposite tendency, since the PHI results are no higher than the preaveraged values. An explanation to this change will be apparent according to an argument that will be given below.

QELS can be used to study both the translational and internal motions of a flexible chain. Thus, the calculation of the translational diffusion coefficient and the longest intramolecular relaxation time, τ_1 , from $S(q, \tau)$ is commonly performed in experimental work. Different elaborated methods have been proposed with this purpose, such as the maximum entropy analysis²⁵ or the widely used CONTIN program.²⁶ These methods usually give a correct separation of the different contributions to $S(q, \tau)$, but the accuracy of their estimations for D_t and τ_1 is not very high, so they cannot discern subtle effects as the influence of preaveraging.

Table VI
Results for D_t and τ_1 Obtained through the Pecora
Analysis of QELS Functions with $x = 1$ ^a

N	FHI		PHI	
	D_t^*	τ_1^*	D_t^*	τ_1^*
6	0.38 ± 0.02	1.37 ± 0.2	0.32 ± 0.02	1.60 ± 0.04
8	0.321 ± 0.005	1.84 ± 0.06	0.28 ± 0.01	2.2 ± 0.1
11	0.29 ± 0.01	3.8 ± 0.8	0.26 ± 0.01	4.11 ± 0.6
15	0.217 ± 0.005	8.2 ± 0.1	0.21 ± 0.01	8.0 ± 0.9
20	0.15 ± 0.02	13 ± 2	0.13 ± 0.03	12 ± 1

^a Calculated from our trajectories for EV chains with FHI and PHI.

Consequently, we have employed a more direct method, based on the expression first proposed by Pecora²⁷ for Gaussian chains

$$S(q, \tau) = e^{-D_t q^2 \tau} [S_0(x) + S_{21}(x)e^{-2\tau/\tau_1} + S_{22}(x)e^{-2\tau/\tau_2} + \dots] \quad (20)$$

The relative amplitudes $S_{lm}(x)$ of the exponential terms in this expression depend strongly on the parameter x . For moderate values of x , such as $x = 1$, only the first two terms in eq 20 are relevant. Consequently, we have tried a fit of our BD results to the form

$$S(q, \tau) = e^{-a\tau} [b_1 + b_2 e^{-d\tau}] \quad (21)$$

by employing a nonlinear least-squares fitting method with a , d , b_1 , and b_2 as adjustable parameters. From the results of these fittings, we have extracted $D_t = a/q^2$ and $\tau_1 = 2/d$. These values are collected in Table VI. It should be pointed out that, as a consequence of employing eq 21 as an approximation, possible contributions of higher relaxation modes characterized by relaxation times τ_k , $k > 1$, are accumulated on τ_1 , and therefore, its value can be considered as a collective intramolecular relaxation time, τ_c , which is the result usually determined from experimental measurements. However, we had noted previously³ that the higher order contributions are almost negligible for $x \simeq 1$.

The results in Table VI have higher uncertainties than those obtained in a similar analysis for Gaussian chains.³ This may be due to the influence of the preexponentials b_1 and b_2 . In the case of Gaussian chains, the Pecora scheme gives theoretical values for these factors that are employed as initial estimations in the nonlinear fittings. However, since we do not have such theoretical predictions for EV chains, we have to use the same initial parameters. Since nonlinear least-squares fitting methods are very sensitive to their given initial estimations, we have found some fluctuations in the results obtained with different trajectories for a given chain.

In spite of this problem, there is a fair agreement between the values of D_t and τ_1 evaluated from the QELS function and those computed directly from the trajectories, through the displacement of the center of masses and the time-correlation function of the Rouse coordinates, according to the methods and results discussed in previous sections. This confirms that the Pecora method to extract D_t and τ_1 from $S(q, \tau)$ is essentially correct even for chains that do not obey the Gaussian statistics. The discrepancies shown in Figure 5 between curves obtained with FHI and PHI mainly reflect the differences for D_t discussed previously (we should remember that the differences in the BD results for D_t obtained from eq 1 with FHI and PHI also showed opposite signs for Gaussian and EV chains). According to that discussion, the differences for EV chains should decrease and change sign to become similar, though slightly smaller than those calculated for

Gaussian chains, as the chain length increases. Then we expect small differences between the FHI and PHI curves in the long-chain limit.

In Figure 5 we have also plotted the curves described by initial slopes corresponding to the cumulants, which have been computed from eqs 12–14. (We have verified for a few illustrative cases that these initial slopes are in good accordance with those obtained directly from the scattering functions, though the latter are associated with higher uncertainties.) It can be observed that the initial slopes are close to the scattering function curves calculated with FHI, while they differ considerably from the functions obtained with PHI. It is not clear whether this trend will be maintained for longer chains since, according to our prediction, the differences between FHI and PHI curves should decrease and change sign as the surface effects (which may be considered practically as finite size effects) vanish. On the contrary, we believe that there will be a region of values of q for which the scattering functions will differ considerably from their initial slopes, as is apparent in the case of Gaussian chains.^{3,28}

Acknowledgment. This work was supported by Grants PB86/0012 (J.J.F.) and PB87/0694 (J.G.T.) from the Dirección General de Investigación Científica y Técnica. A.R. acknowledges a Fellowship from the Plan de Formación del Personal Investigador.

References and Notes

- Doi, M.; Edwards, S. F. *The Theory of Polymer Dynamics*; Oxford Science: Oxford, U.K., 1989.
- Allison, S. A.; McCammon, J. A. *Biopolymers* **1984**, *23*, 363.
- Rey, A.; Freire, J. J.; Garcia de la Torre, J. *J. Chem. Phys.* **1989**, *90*, 2033.
- Allison, S. A.; Sorlie, S. S.; Pecora, R. *Macromolecules* **1990**, *23*, 1110.
- Fixman, M. *J. Chem. Phys.* **1983**, *78*, 1594.
- Bishop, M.; Clarke, J. H. R. *J. Chem. Phys.* **1989**, *90*, 6647.
- Yamakawa, H. *Modern Theory of Polymer Solutions*; Harper and Row: New York, 1971.
- Downey, J. P.; Crabb, C. C.; Kovac, J. *Macromolecules* **1986**, *19*, 2202.
- Fixman, M. *J. Chem. Phys.* **1983**, *78*, 1588.
- Rey, A.; Freire, J. J.; Garcia de la Torre, J. Submitted for publication in *Polymer*.
- Rotne, J.; Prager, S. *J. Chem. Phys.* **1969**, *50*, 4831.
- Yamakawa, H. *J. Chem. Phys.* **1970**, *53*, 436.
- Daoud, M.; Cotton, J. P.; Farnoux, B.; Jannick, G.; Sarma, G.; Benoit, H.; Duplessix, R.; Picot, C.; de Gennes, P. G. *Macromolecules* **1975**, *8*, 804.
- Semlyen, J. A. In *Cyclic Polymers*; Semlyen, J. A., Ed.; Elsevier: London, 1986.
- Zimm, B. H. *Macromolecules* **1980**, *13*, 592.
- Garcia Bernal, J. M.; Tirado, M. M.; Freire, J. J.; Garcia de la Torre, J. *Macromolecules* **1991**, *24*, 593.
- Fixman, M. *J. Chem. Phys.* **1986**, *84*, 4085.
- Wang, S.-Q.; Douglas, J. F.; Freed, K. F. *Macromolecules* **1985**, *18*, 2464.
- Akcasu, Z.; Gurol, H. *J. Polym. Sci., Polym. Phys. Ed.* **1976**, *14*, 1.
- Burchard, W.; Schmidt, M.; Stockmayer, W. H. *Macromolecules* **1980**, *13*, 580.
- Benmouna, M.; Akcasu, A. Z. *Macromolecules* **1980**, *13*, 409.
- Benmouna, M.; Akcasu, A. Z. *Macromolecules* **1978**, *11*, 1187.
- Berne, R.; Pecora, R. *Dynamic Light Scattering*; Wiley: New York, 1976.
- Pecora, R. *J. Chem. Phys.* **1965**, *43*, 1562.
- Livesey, A. K.; Licinio, P.; Delaye, M. *J. Chem. Phys.* **1986**, *84*, 5102.
- Provencher, S. W. *Comput. Phys. Commun.* **1982**, *27*, 213.
- Pecora, R. *J. Chem. Phys.* **1968**, *49*, 1032.
- Escudero, J. A.; Freire, J. J. *Polym. J.* **1982**, *14*, 277.